Supplemental material for:

An absence of nuclear lamins in keratinocytes leads to ichthyosis, defective epidermal barrier function, and intrusion of nuclear membranes and endoplasmic reticulum into the nuclear chromatin

Hea-Jin Jung *et al.*

SUPPLEMENTAL METHODS

Sterol measurement

The epidermis of newborn mice was isolated as described (see *Studies with primary keratinocytes*), snap-frozen, and stored at –80°C until all samples were ready for analysis. Sterol levels were measured as described previously (1). Briefly, skin samples were boiled in highly basic methanol to extract bulk lipids. Extracts were then hydrolyzed with 10N KOH and the sterol-containing fraction isolated by chromatography on aminopropyl SPE (solid-phase extraction) columns. Individual sterols were resolved on C_{18} core-shell HPLC columns and quantified on triple quadrupole mass spectrometers. For each sample, the equivalent of 4 mg of tissue was analyzed.

Studies with immortalized MEFs

Immortalized MEFs were seeded in 6-well plates at 10,000 cells per well in the morning and cultured in DMEM medium with 10% FBS at 37°C with 5% CO_2. In the evening of the same day, the cells were rinsed with Opti-MEM I Reduced Serum Medium (Gibco) and incubated with adenovirus (Ad-CMV-Cre and Ad-CMV-β-Gal; Vector Biolabs) diluted in Opti-MEM I Reduced Serum Medium at 500 MOI overnight. The next morning, the medium was changed (DMEM medium with 10% FBS). On day 6, the cells

were seeded in 6-well plates at 10,000 cells/well and transduced again. When the cells became confluent on day 12, they were split once again.

For BrdU pulse-labeling studies, cells were seeded on coverslips in 24-well plates and cultured in DMEM medium with 10% FBS at 37°C with 5% CO_2. The next day, BrdU was added to the medium at a final concentration of 10 μM. After 4 h, the cells were fixed with 4% PFA, permeabilized with 0.1% Triton X-100 in PBS containing 1 mM $CaCl_2$ and 1 mM $MgCl_2$, pretreated with 1N and 2N HCl, neutralized in 0.1 M sodium borate (pH 8.5), and blocked with PBS containing 1 mM $CaCl_2$, 1 mM $MgCl_2$, 10% fetal bovine serum, and 0.2% bovine serum albumin. The following primary antibodies were used: a goat polyclonal antibody against lamin B1 (1:400) (sc-6217; Santa Cruz); a rabbit polyclonal antibody against lamin C (1:200) (LS-B2972, Lifespan Biosciences); and a rat monoclonal antibody against BrdU (1:200) (ab6326, Abcam). Alexa Fluor–labeled donkey antibodies against goat, rabbit, or rat IgG (Invitrogen) were used to detect binding of primary antibodies.

REFERENCES

1. **McDonald JG, Smith DD, Stiles AR, Russell DW.** 2012. A comprehensive method for extraction and quantitative analysis of sterols and secosteroids from human plasma. J Lipid Res **53:**1399-1409.

2. **Radner FP, Grond S, Haemmerle G, Lass A, Zechner R.** 2011. Fat in the skin: Triacylglycerol metabolism in keratinocytes and its role in the development of neutral lipid storage disease. Dermatoendocrinol **3:**77-83.

3. **Geiger SK, Bar H, Ehlermann P, Walde S, Rutschow D, Zeller R, Ivandic BT, Zentgraf H, Katus HA, Herrmann H, Weichenhan D.** 2008. Incomplete

nonsense-mediated decay of mutant lamin A/C mRNA provokes dilated cardiomyopathy and ventricular tachycardia. J Mol Med (Berl) **86:**281-289.

SUPPLEMENTAL FIGURES

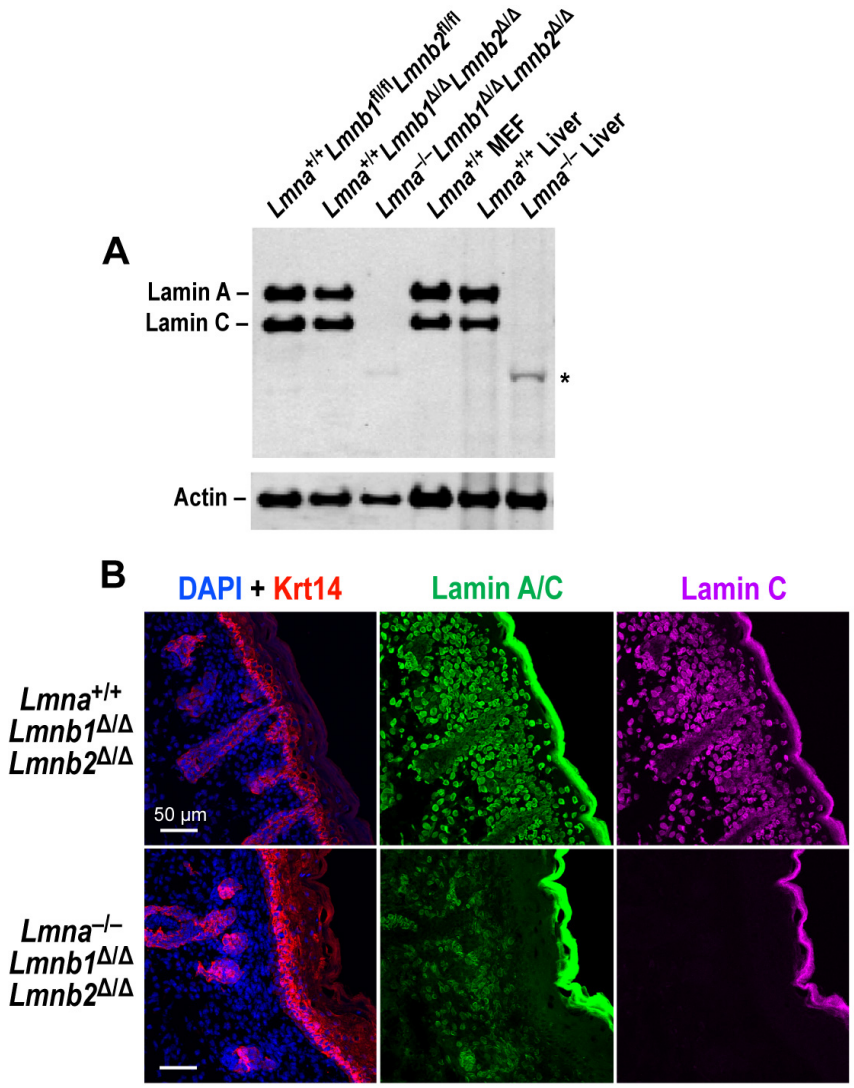

Figure S1. Detection of trace amounts of an internally truncated prelamin A protein in primary keratinocytes and skin sections from *Lmna*$^{-/-}$*Lmnb1*$^{\Delta/\Delta}$*Lmnb2*$^{\Delta/\Delta}$ mice. (A) Western blot analysis of lamin A/C expression in primary keratinocytes with a goat polyclonal antibody against lamin A/C. The asterisk indicates a protein band with a molecular weight corresponding to the truncated prelamin A reported earlier (2). (B) Immunohistochemistry of skin sections from newborn *Lmna*$^{+/+}$*Lmnb1*$^{\Delta/\Delta}$*Lmnb2*$^{\Delta/\Delta}$ and *Lmna*$^{-/-}$*Lmnb1*$^{\Delta/\Delta}$*Lmnb2*$^{\Delta/\Delta}$ mice with antibodies against Krt14 (red), the N-terminal region (the first eight amino acids of the non-alpha-helical head domain) of lamin A/C (3) (green), and lamin C (magenta). DNA was stained with DAPI (blue). Scale bar, 50 µm.

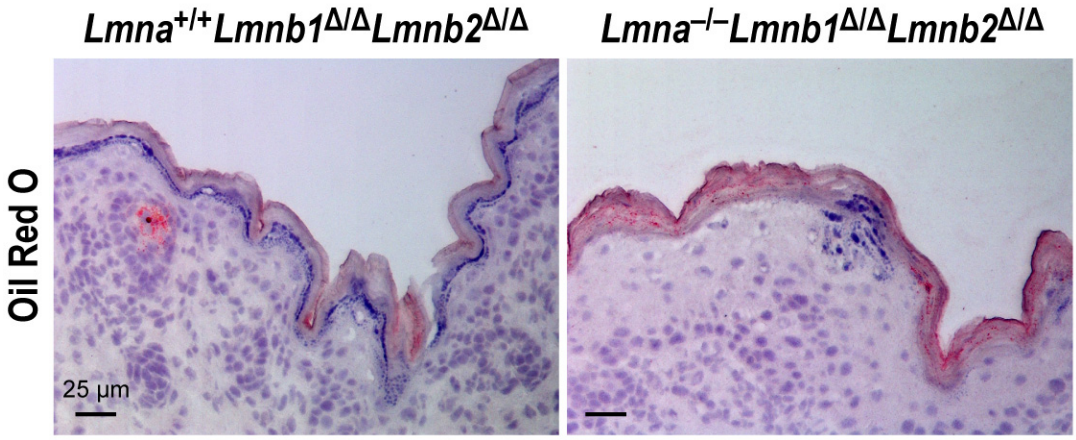

Figure S2. Oil red O staining of skin sections from newborn *Lmna*$^{+/+}$*Lmnb1*$^{\Delta/\Delta}$*Lmnb2*$^{\Delta/\Delta}$ and *Lmna*$^{-/-}$*Lmnb1*$^{\Delta/\Delta}$*Lmnb2*$^{\Delta/\Delta}$ mice. The sections were counterstained with hematoxylin. Scale bar, 25 μm. Many oil red O positive lipid droplets were identified in the stratum corneum of *Lmna*$^{-/-}$*Lmnb1*$^{\Delta/\Delta}$*Lmnb2*$^{\Delta/\Delta}$ mice.

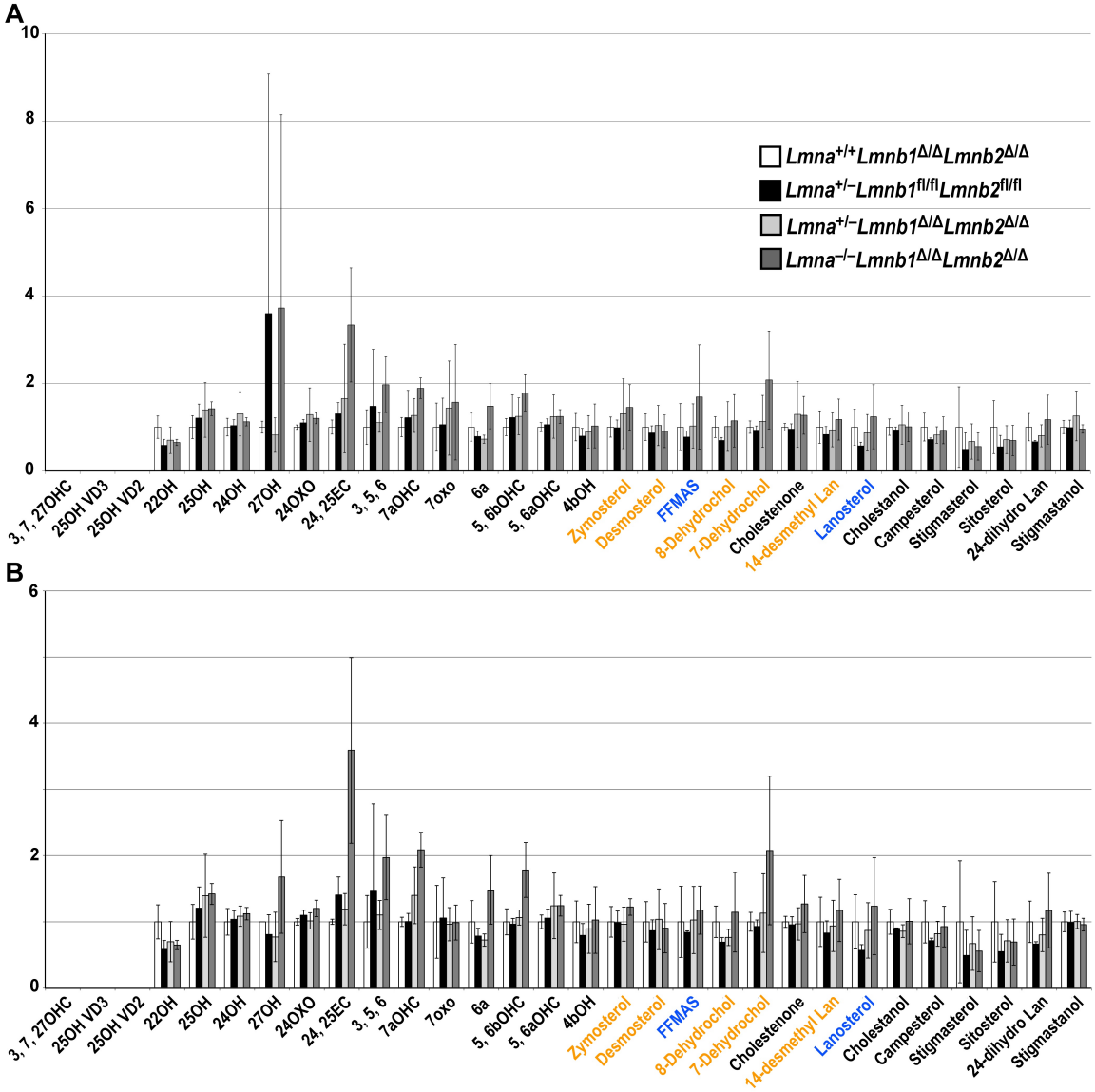

Figure S3. No significant changes in sterol levels in the epidermis of newborn *Lmna*$^{-/-}$ *Lmnb1*$^{\Delta/\Delta}$*Lmnb2*$^{\Delta/\Delta}$ mice. (A) The levels of multiple sterol intermediates, including those before (blue) or after (orange) the Δ^{14}-reductase–mediated step, were measured by mass spectrometry (1). Values represent mean ± SD. *Lmna*$^{+/+}$*Lmnb1*$^{\Delta/\Delta}$*Lmnb2*$^{\Delta/\Delta}$, n = 5; *Lmna*$^{+/-}$*Lmnb1*$^{fl/fl}$*Lmnb2*$^{fl/fl}$, n = 4; *Lmna*$^{+/-}$*Lmnb1*$^{\Delta/\Delta}$*Lmnb2*$^{\Delta/\Delta}$, n = 5; *Lmna*$^{-/-}$ *Lmnb1*$^{\Delta/\Delta}$*Lmnb2*$^{\Delta/\Delta}$, n = 5. (B) Re-analysis of the data reported in panel A after excluding potential outliers as judged by Grubb's test ($p < 0.05$). No more than one sample per genotype was excluded.

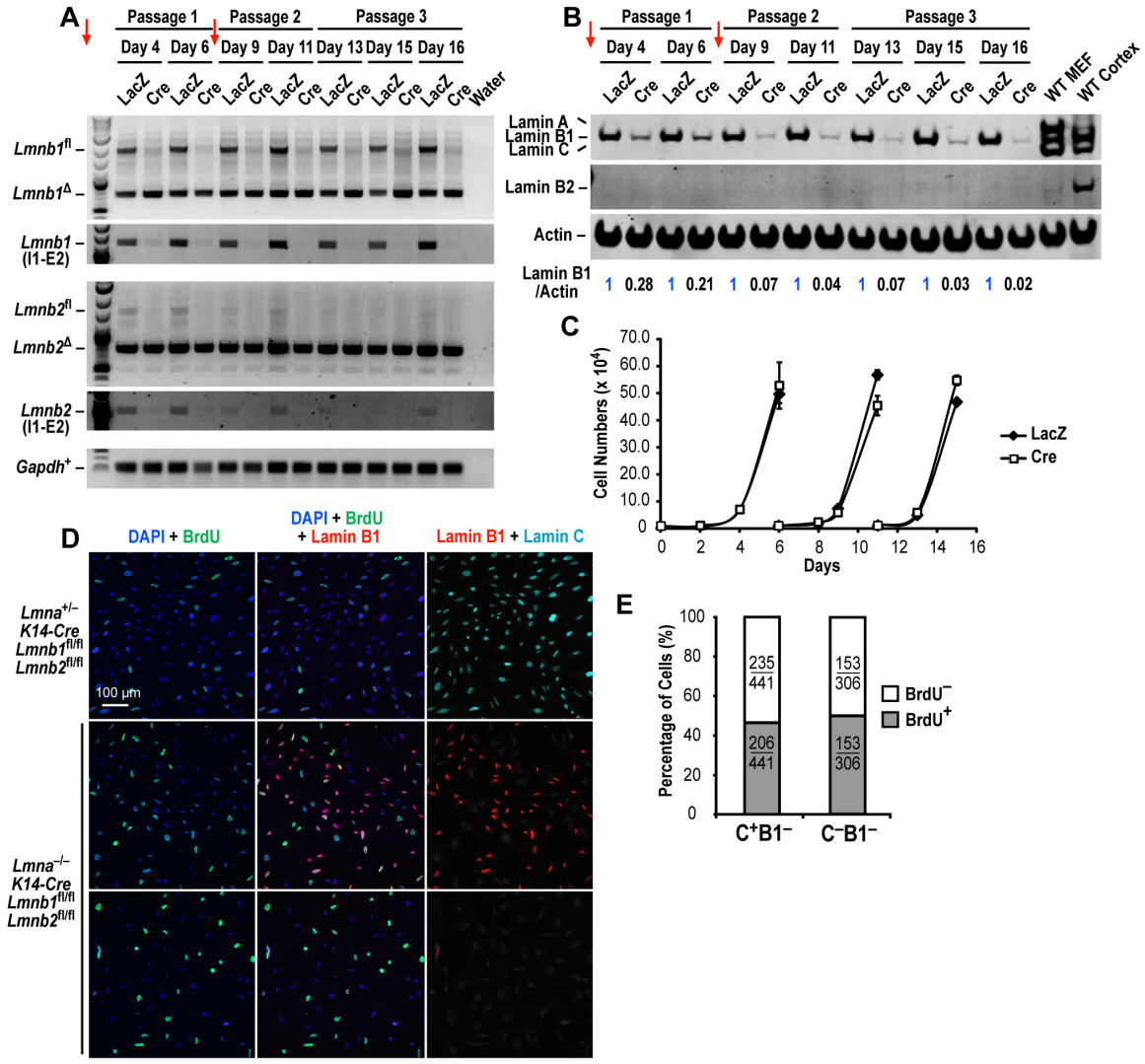

Figure S4. Normal cell proliferation in fibroblasts lacking nuclear lamins. (A–C) Cell proliferation assays with immortalized *Lmna*$^{-/-}$*Lmnb1*$^{fl/fl}$*Lmnb2*$^{fl/fl}$K14-Cre mouse embryonic fibroblasts (MEFs). MEFs were transduced with either *lacZ* or *Cre* adenovirus and monitored over three passages for changes in genotype (A), nuclear lamin protein expression (B), and growth rate (C). In these studies, we observed *Lmnb1* and *Lmnb2* delta recombination alleles at baseline, even before adenoviruses were given, due to unexpected expression of the K14-*Cre* transgene in fibroblasts. To achieve more complete recombination, the cells were treated with *Cre*-adenovirus (or *LacZ*-adenovirus as a control) at day 0 and day 6 (red arrows). The experiment was performed in triplicate. (A) Changes in *Lmnb1* and *Lmnb2* genotypes were monitored with primers flanking the

floxed segments of the gene; these reactions detected the floxed allele (fl) and the deletion allele (Δ). We also amplified segments across the 5′ end of the floxed region of each gene (I1–E2). *Gapdh* was used as a normalization control. (B) Western blot analysis of lamins B1 and B2 expression in the transduced MEFs. The levels of lamin B1 were normalized to the levels of actin and expressed relative to *LacZ*-transduced cells (set at a value of one). The values are reported at the bottom. Lamin B2 expression was barely detectable in these fibroblasts. (C) Growth rate of fibroblasts that had been treated with *Cre*- or *LacZ*-adenoviruses. Values represent the mean ± SD. (D) BrdU labeling studies with immortalized $Lmna^{+/-}Lmnb1^{\Delta/\Delta}Lmnb2^{\Delta/\Delta}$ and $Lmna^{-/-}Lmnb1^{\Delta/\Delta}Lmnb2^{\Delta/\Delta}$ MEFs (one line with modest levels of recombination and retention of lamin B1 synthesis, and another line with substantial levels of baseline recombination and little lamin B1 synthesis). BrdU was added to the culture medium and the cells were analyzed for BrdU uptake 4 h later by immunofluorescence microscopy. Cells were stained for BrdU (green), lamin B1 (red), and lamin C (cyan). DNA was stained with DAPI (blue). Scale bar, 100 μm. (E) Quantification of_BrdU-positive cells in lamin B1–deficient $Lmna^{+/-}Lmnb1^{\Delta/\Delta}Lmnb2^{\Delta/\Delta}$ cells ($C^{+}B1^{-}$) and $Lmna^{-/-}Lmnb1^{\Delta/\Delta}Lmnb2^{\Delta/\Delta}$ cells ($C^{-}B1^{-}$) (see panel D). >300 cells/genotype ($n = 2$) were quantified in a blinded fashion.

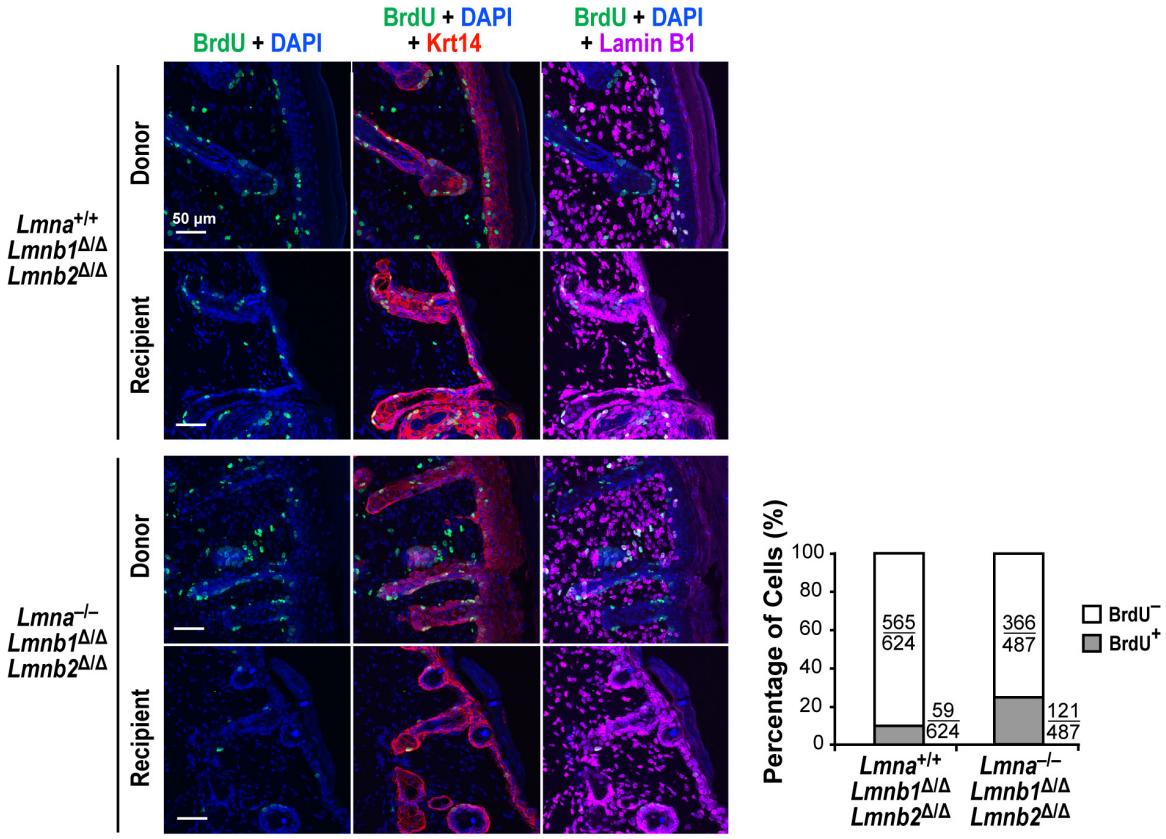

Figure S5. BrdU labeling studies in *Lmna*$^{+/+}$*Lmnb1*$^{\Delta/\Delta}$*Lmnb2*$^{\Delta/\Delta}$ and *Lmna*$^{-/-}$ *Lmnb1*$^{\Delta/\Delta}$*Lmnb2*$^{\Delta/\Delta}$ skin grafts. Recipient mice were given an intraperitoneal injection of BrdU 10 days after the surgery; BrdU incorporation was assessed 6 h later. Skin sections were stained with antibodies against BrdU (green), Krt14 (red), and lamin B1 (magenta). DNA was visualized with DAPI (blue). No differences were observed. Scale bar, 50 μm. The percentage of BrdU-positive cells was assessed in >450 donor epidermal keratinocytes/genotype (*Lmna*$^{+/+}$*Lmnb1*$^{\Delta/\Delta}$*Lmnb2*$^{\Delta/\Delta}$, $n = 3$; *Lmna*$^{-/-}$*Lmnb1*$^{\Delta/\Delta}$*Lmnb2*$^{\Delta/\Delta}$, $n = 2$) in a blinded fashion; results are shown on the right.

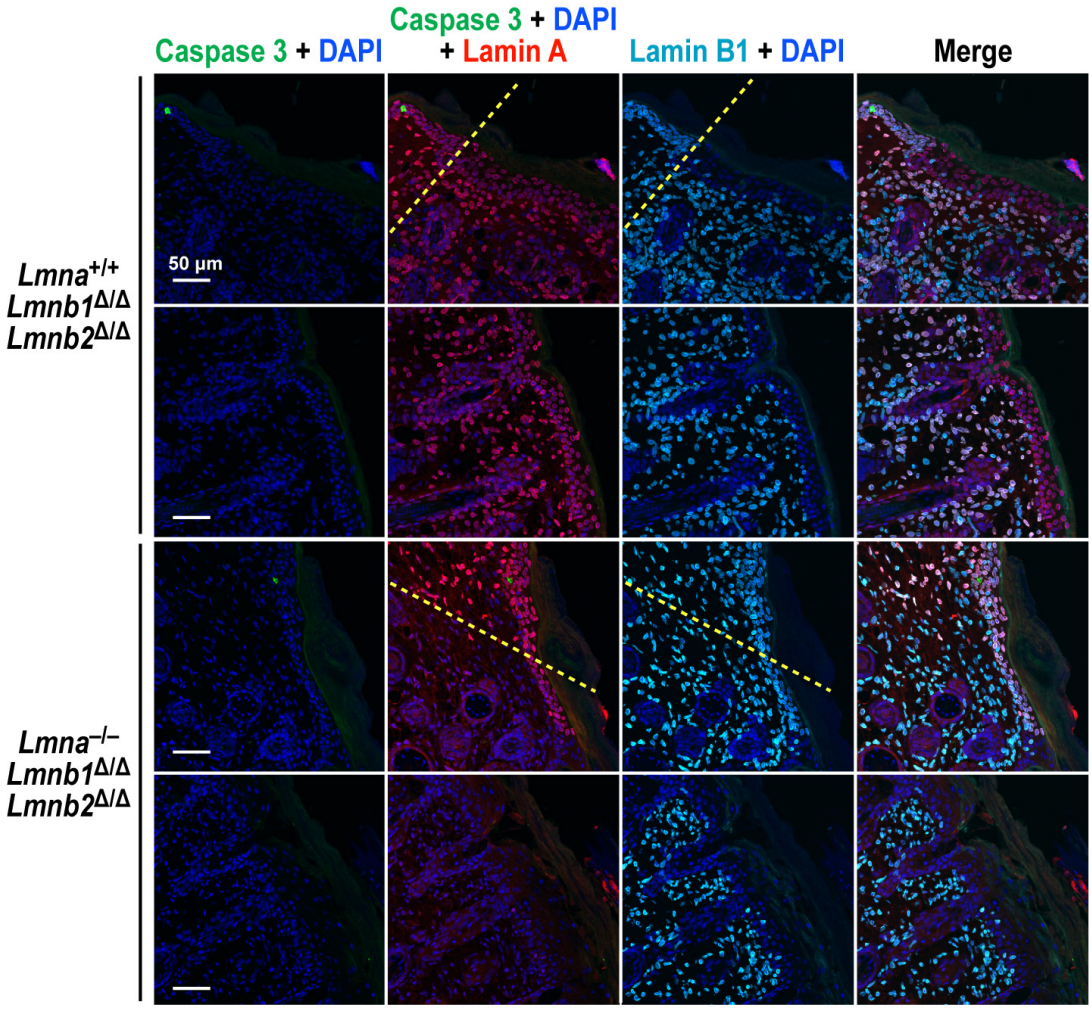

Figure S6. Immunofluorescence microscopy on sections from *Lmna*$^{+/+}$*Lmnb1*$^{\Delta/\Delta}$*Lmnb2*$^{\Delta/\Delta}$ and *Lmna*$^{-/-}$*Lmnb1*$^{\Delta/\Delta}$*Lmnb2*$^{\Delta/\Delta}$ skin grafts that had been stained with antibodies against caspase 3 (green), lamin A (red), and lamin B1 (cyan). DNA was stained with DAPI (blue). The boundary between the donor skin and the grafts is indicated with yellow dashed lines. The graft is located below the dashed lines. Caspase 3–positive cells were extremely rare in skin grafts, regardless of the genotype of the grafted skin. Scale bar, 50 μm.

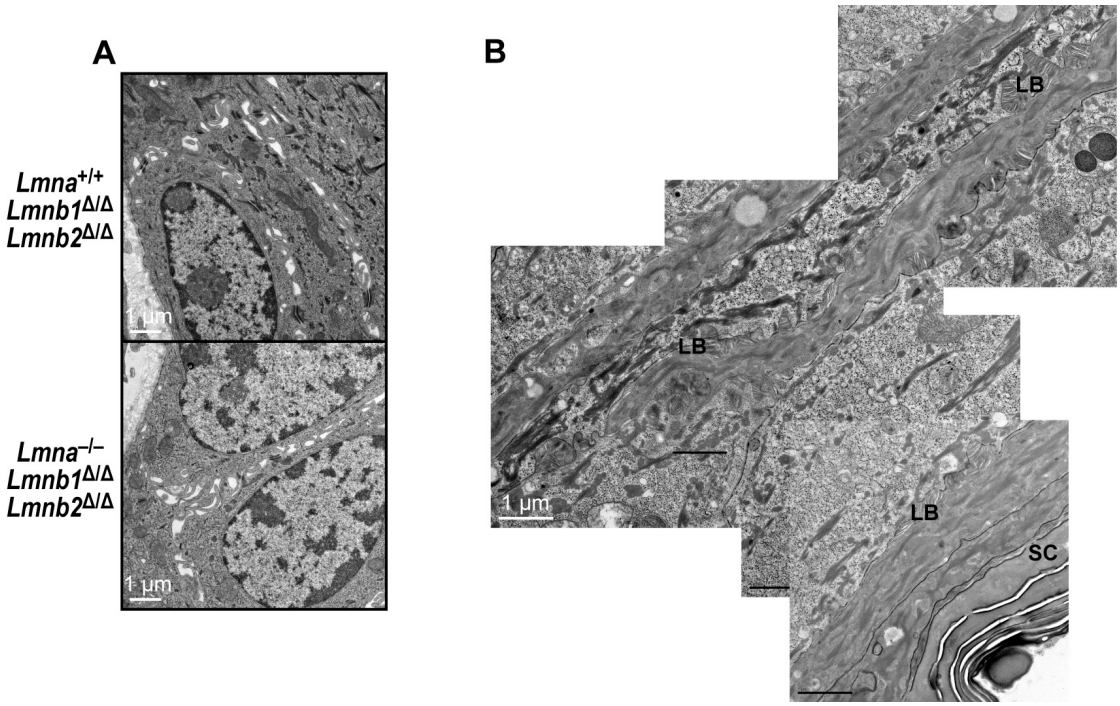

Figure S7. Electron micrographs of keratinocytes and lamellar bodies in the skin from *Lmna*$^{-/-}$*Lmnb1*$^{\Delta/\Delta}$*Lmnb2*$^{\Delta/\Delta}$ mice. (A) Images of occasional *Lmna*$^{-/-}$*Lmnb1*$^{\Delta/\Delta}$*Lmnb2*$^{\Delta/\Delta}$ keratinocytes with normal nuclear morphology. Scale bar, 1 μm. (B) Composite of multiple electron micrographs showing lamellar bodies in the interspersed regions of stratum granulosum and stratum corneum in *Lmna*$^{-/-}$*Lmnb1*$^{\Delta/\Delta}$*Lmnb2*$^{\Delta/\Delta}$ mice. SC, stratum corneum; LB, lamellar bodies. Scale bar, 1 μm.

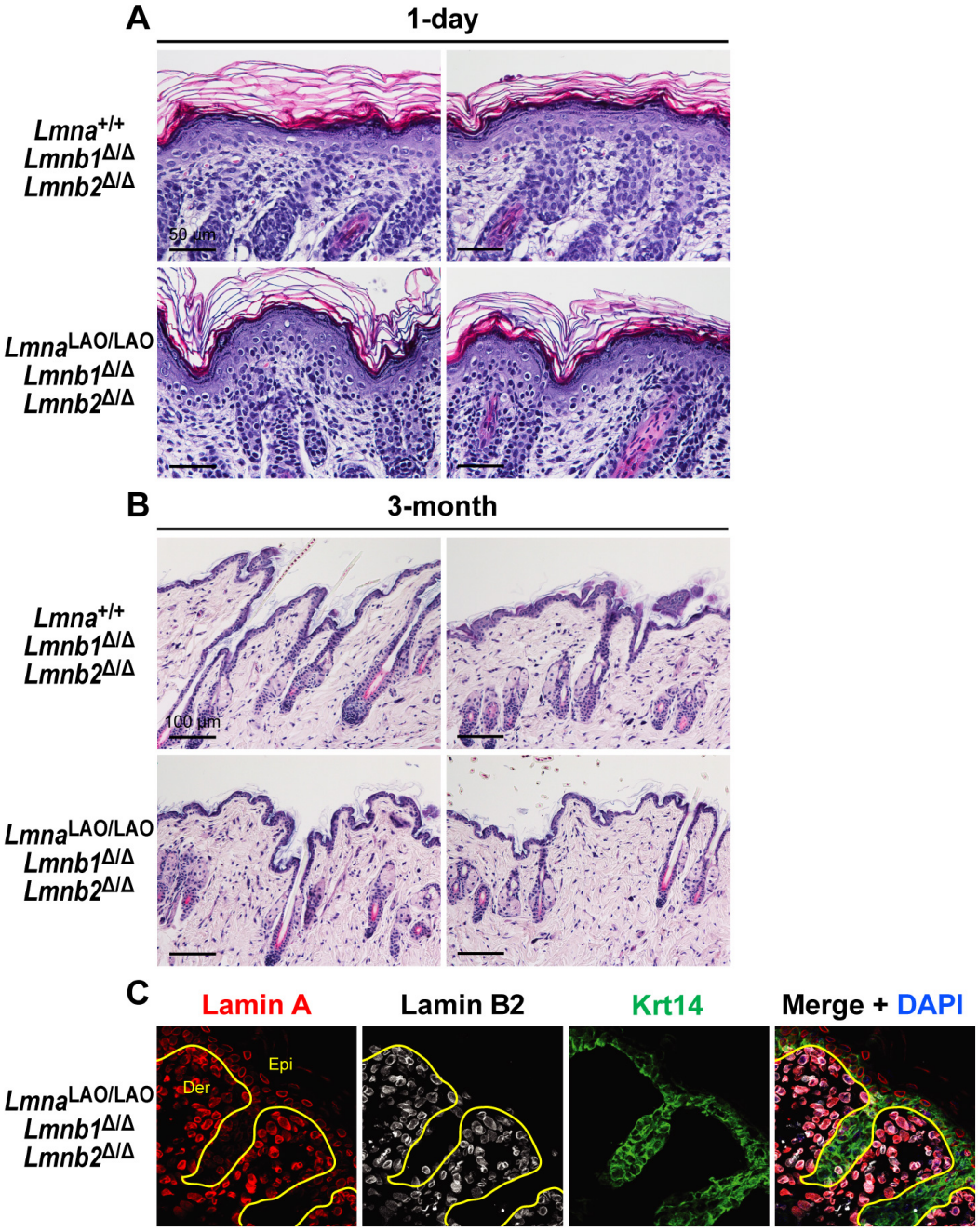

Figure S8. Normal development of skin and hair in *Lmna*$^{LAO/LAO}$*Lmnb1*$^{Δ/Δ}$*Lmnb2*$^{Δ/Δ}$ mice. Skin sections from newborn (A) and 3-mo-old (B) *Lmna*$^{+/+}$*Lmnb1*$^{Δ/Δ}$*Lmnb2*$^{Δ/Δ}$ and *Lmna*$^{LAO/LAO}$*Lmnb1*$^{Δ/Δ}$*Lmnb2*$^{Δ/Δ}$ mice were stained with H&E. Scale bar, 50 μm (A); 100 μm (B). (C) Immunohistochemistry of skin sections from a *Lmna*$^{LAO/LAO}$*Lmnb1*$^{Δ/Δ}$*Lmnb2*$^{Δ/Δ}$ mouse with antibodies against lamin A (red), lamin B2 (white), and Krt14 (green). DNA was stained with DAPI (blue). The boundary between the epidermis (Epi) and dermis (Der) is indicated with yellow lines.

3,7,27OHC	LMST04030178	7aOHC	LMST01010013	7-Dehydrochol	LMST01010069
25OH VD3	LMST03020246	7oxo	LMST01010049	Cholestenone	LMST01010015
25OH VD2	LMST03010030	6a	LMST01010135	14-desmethyl Lan	LMST01010176
22OH	LMST01010086	5,6bOHC	LMST01010010	Lanosterol	LMST01010017
25OH	LMST01010018	5,6aOHC	LMST01010011	Cholestanol	LMST01010077
24OH	LMST01010019	4bOH	LMST01010014	Campesterol	LMST01030097
27OH	LMST01010057	Zymosterol	LMST01010066	Stigmasterol	LMST01040124
24OXO	LMST01010133	Desmosterol	LMST01010016	Sitosterol	LMST01040129
24,25 EC	LMST01010012	FFMAS	LMST01010149	24-dihydro Lan	LMST01010087
3,5,6	LMST01010052	8-Dehydrochol	LMST01010242	Stigmastanol	LMST01040128

Table S1. LIPID MAPS IDs of the sterol lipids analyzed in Fig. S3 (http://www.lipidmaps.org/).